

DOI: 10.58240/1829006X-2025.21.10-322



## ORIGINAL RESEARCH

## EVALUATION AND AUTOMATED SEGMENTATION OF THE NASOPALATINE CANAL USING CBCT AND DEEP LEARNING (U-NET) ARCHITECTURE

Merna Shabo Yousif<sup>1</sup> B.D.S, Saleem Khadir Musalah<sup>2</sup> CABMS<sup>1</sup> Department of Oral surgery, College of Dentistry University of Duhok, Duhok, Iraq Email: [merna275yousif@gmail.com](mailto:merna275yousif@gmail.com) (corresponding author) ORCID: <https://orcid.org/0009-0000-6649-6246><sup>2</sup> Department of radiology, college of medicine University of Duhok, Duhok, Iraq. Email: [Saleem.musalah@uod.ac](mailto:Saleem.musalah@uod.ac) ORCID: <https://orcid.org/0009-0000-4191-0711>**Corresponding author:** Merna Shabo Yousif Department of Oral surgery, College of Dentistry University of Duhok, Duhok, Iraq Email: [merna275yousif@gmail.com](mailto:merna275yousif@gmail.com) (corresponding author) ORCID: <https://orcid.org/0009-0000-6649-6246>**Received:** Sep 7, 2025; **Accepted:** Oct 29, 2025; **Published:** Nov. 10 2025

## ABSTRACT

**Background:** Background and Objective: The nasopalatine canal (NPC) is an important structure in maxillofacial surgery and dentistry, and has implications for surgical and dental treatments. This study aimed to assess morphological differences and anatomical dimensions of the NPC with cone-beam computed tomography (CBCT) and to investigate the usefulness of deep learning with U-Net architecture, in the automated segmentation of the canal.

**Methods:** 441 adult CBCT scans were studied in a retrospective cross-sectional manner. NPC was evaluated in sagittal view to determine the shape, length, and width at three levels, as well as age-related changes. After evaluation, sagittal images were extracted. An artificial intelligence (AI) model based on U-Net, trained from manually annotated data, was then applied for segmentation. The model was evaluated using metrics such as the Dice score, accuracy, precision, recall, and F1 score.

**Results:** Cylindrical and funnel shapes were the most common across all age groups, with no significant difference in shape distribution between the two groups. NPC width did not significantly change with age, but canal length significantly increased with age ( $P = 0.0003$ ). For the U-Net model, Class 2 demonstrated higher training performance compared to the others (Dice = 0.531, Recall = 0.682). In the testing phase, Class 3 demonstrated the highest Dice value (0.868) and accuracy (1.000); whereas Class 4 had the lowest accuracy (Dice = 0.263, Accuracy = 0.790).

**Conclusion:** CBCT can provide detailed evaluation of the NPC morphology. The U-Net-based AI model demonstrated substantial performance in segmenting the NPC. Combining AI with CBCT could improve diagnostic accuracy and treatment planning in maxillofacial surgeries.

**Keywords:** Nasopalatine canal, Cone beam computed tomography, Artificial intelligence, U-Net Segmentation, Anatomical Variations

## INTRODUCTION

The nasopalatine canal, or incisive canal, is located in the anterior aspect of the hard palate behind the maxillary incisors, which serves as a pathway from the oral to the nasal cavity. It contains soft tissue and neurovascular structures; namely, the nasopalatine nerve and the sphenopalatine artery that runs along its length<sup>1</sup>.

The NPC was described in full detail for the first time

by Stenson in 1683. The mouth opening of the NPC is situated beneath the incisive papilla as incisive foramen and the canal -ends in the nasal cavity via the Stensen's foramina<sup>2,3</sup>. The anterior maxillary area is one of the most important site in esthetic rehabilitation and the most common view of dental trauma and tooth loss. Implant placement in this region should be critically evaluated for the nasopalatine canal in order to avoid problems such as hemorrhage, pain,

paresthesia and implant loss<sup>4,5</sup>.

Traditional imaging tools were used previously to evaluate the canal such as intraoral radiography, panoramic imaging, and CT, which were disturbed by distortion, superimposition, and low resolution. The introduction of CBCT, which provides 3D, high-resolution, multiplanar imaging with lower doses of radiation compared to conventional CT, revolutionized diagnostic imaging. Its rapid scanning, reduced radiation exposure, and higher comfort for the patient makes CBCT more appropriate for maxillofacial area<sup>6</sup>.

Advances in the field of AI specifically the development of deep learning techniques, for instance, U-Net have facilitated automated CBCT image analysis in dentistry for segmentation of anatomical structures, such as mandibular canal, maxillary sinus, and possibly the nasopalatine canal. These technologies are promising for increasing diagnostic precision and decreasing clinician workload in maxillofacial imaging<sup>7</sup>.

Nowadays, the application of deep learning technology in medical imaging has attracted extensive attention. How to automatically recognize and segment the lesions in medical images has become one of the issues that concern lots of researchers, medical image segmentation is a fundamental task in clinical radiology, critical for both diagnostic and therapeutic processes<sup>8</sup>.

The purpose of the present study was to evaluate the anatomic characteristic of the NPC by CBCT regarding its morphological features, size, and clinical significance. It also considers the use of artificial intelligence specifically deep learning (U-Net) models for automated segmentation of the NPC. Fusion of CBCT imaging with big-data AI analysis is envisioned to improve diagnostic accuracy, decrease clinician workload, and enable safer and personalized treatment planning in maxillofacial surgery.

## MATERIALS AND METHODS

This was a retrospective cross-sectional study and was carried out in the X-ray department of the private clinics in Duhok, Iraq. The scans were obtained for diagnostic and treatment planning purposes and were anonymized prior to analysis to ensure patient confidentiality. From 600 adult CBCT scans, 441 subjects (221 males, 220 females) complied with the inclusion criteria. The age of participants ranged from 18 to 80 years and were grouped into five age groups. The sample size dimension was determined according

previous CBCT studies on NPC morphology and allowed age-stratification (subgroup analysis):

- Group 1: 18–30 years
- Group 2: 31–40 years
- Group 3: 41–50 years
- Group 4: 51–60 years
- Group 5: Above 60 years

Only patients over 18 years old were enrolled in this study; they also had to have lateral and central maxillary incisor present. Exclusion criteria were poor-quality CBCT images or with technical problems and involving the image clarity, lack of any maxillary incisor, and pathological condition in location of NPC including nasopalatine duct cysts, tumors, cleft lip, and periodontal diseases. Patients with orthodontic appliances or metal restorations in the anterior maxilla and with dental implants, bone grafts or dentition with spaces in the anterior maxilla were also excluded. Furthermore, cases where impaction teeth close to the NPC, such as impacted canines, were not included in the study.

The sagittal view of the CBCT will be used for measurements of the NPC (Figure 1). Length is the distance measured along the trajectory to the incisive foramen from the start of canal in the floor of nasal cavity. Width will be evaluated at three aspects (superior, middle, and inferior), by the distance of the horizontal distance between the walls of the canal in these same points. All measurements will be expressed in millimeters.

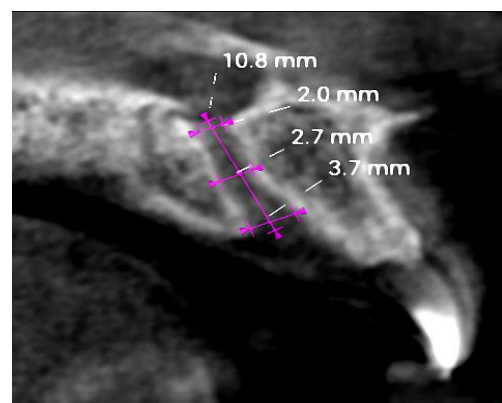


**Figure 1.** Measuring the length and width of the canal and recorded in (mm).

According to its shape in the sagittal view, the NPC will be differentiated into four shapes (Figure 2):

1. Cylindrical – uniform diameter throughout.
2. Funnel – narrow at the top, widening toward the bottom.
3. Hourglass – wider at both ends with a narrow middle.
4. Spindle – The NPC is thicker in its middle section than at its top or bottom.

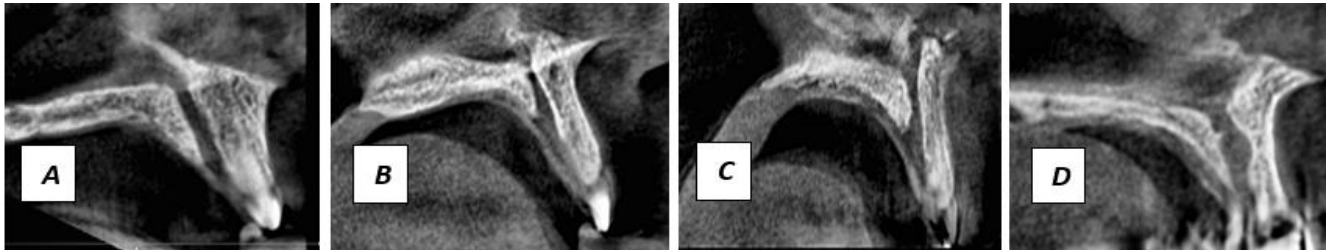


**Figure 2.** Morphology of the nasopalatine canal in sagittal view (A-Cylindrical, B-Funnel, C-Hourglass, D-Spindle)

After canal assessment, sagittal view images were selected for the designing of an AI model designed for shape assessment of the virtual canal.

The CBCT images were manually annotated to create ground-truth labels for model training and evaluation. Labeling was performed using *MakeSense.ai*. Two experienced oral and maxillofacial radiologists, each with more than 10 years of clinical experience, independently evaluated the images and segmented the nasopalatine canal (NPC) in each scan.

Each part of the canals is colored by using unique RGB colors. These are converted into class numbers (1 to 4) as follows:

- Class 1 : hourglass shape ( blue)
- Class 2 : cylindrical shape ( green)
- Class 3 : spindle shape ( red)
- Class 4 : funnel shape ( turquoise)

while background is labeled as 0 as show in (Figure 3). This step allows the AI model to learn each canal part's structure and location individually.

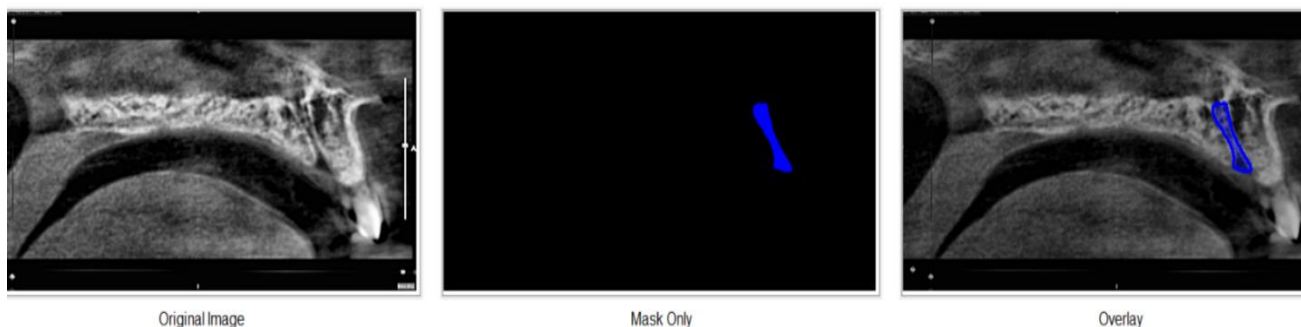


**Figure 3.** The figure illustrates the AI-based segmentation process of the nasopalatine canal in sagittal CBCT images: first the original CBCT image, in the middle the segmentation mask generated by the AI model, and then the overlay of the mask on the original image showing the detected canal region.

A few preprocessing procedures were applied to improve the image quality and the visibility of the canals before training the AI model, i.e.:

- Grayscale transformation: structure-based focus.
- CLAHE for contrast enhancement.
- Bilateral filter to remove noise with edge remainence
- Sharpening to define canal boundaries.
- Normalization of pixel values.
- Auto-cropping for the area of interest, and
- Resizing all images to the size 512×256 pixels.

The dataset was segmented into the following three parts after preprocessing:

- 80% for Training: This part is for teaching the AI to recognize the canal
- 10% for Validation: This portion is applied in training process to observe model performance and avoid overfitting
- 10% for Testing: By the time training is finished, these images are employed to do a last accuracy check of the AI model.

The deep learning architecture applied is U-Net model, which is designed towards medical image segmentation. U-Net provides the best trade-off between accuracy, computing load and detail preservation, so that it is the most suitable model to segment the nasopalatine canal.

To measure performance, various metrics were used:

- **Dice Score:** Measures overlap between predicted and actual canal.
- **Accuracy:** Percentage of correct pixel predictions.
- **Precision:** How many predicted canal pixels were actually correct.
- **Recall:** How many actual canal pixels were detected.
- **F1 Score:** A balance between precision and recall.

A U-Net architecture was implemented for 2D CBCT slice segmentation of the NPC. The model consists of an encoder with four down-sampling steps and a decoder with four up-sampling steps, with skip connections between corresponding layers. Input images were 512×256 pixels, and each convolutional block consisted of two 3×3 convolutional layers followed by ReLU activation. The model was trained using the Adam optimizer with a learning rate of 0.0001, a batch size of 8, and Dice loss as the objective function. Early stopping was applied to prevent overfitting. For Statistical analysis age were presented as mean (SD) or n (%), as appropriate. Normality of age and NPC shapes in sagittal planes was assessed using Q-Q plots. Variations in NPC shapes by age were analyzed using Pearson chi-squared tests. Independent t-tests or one-way ANOVA were used to compare sagittal shapes, with Tukey tests for pairwise age group comparisons of NPC length. A p-value <0.05 was considered significant. Analyses were performed using JMP, Version 18.0 (SAS Institute Inc., Cary, NC, 1989–2023).

**RESULTS**

In (Table 1) No significant differences of NPC shape distribution were observed in the sagittal plane among the age groups. The cylindrical shape was the most common in all age groups, 31.82-42.19%, followed by funnel shape. Some differences were observed for the hourglass and spindle forms, but without statistical significance.

**Table 1. Comparison of various shapes of NPCs in sagittal plane between age groups**

Shapes of the NPC	Age groups					P
	18-30 (n=119)	31-40 (n=64)	40-50 (n=110)	51-60 (n=83)	more than 60 (n=65)	
<b>Sagittal plane shape</b>						
<b>Hourglass</b>	28 (23.53)	12 (18.75)	26 (23.64)	12 (14.46)	10 (15.38)	0.3590
<b>Cylindrical</b>	46 (38.66)	27 (42.19)	35 (31.82)	31 (37.35)	22 (33.85)	0.6635
<b>Spindle</b>	9 (7.56)	6 (9.38)	15 (13.64)	14 (16.87)	9 (13.85)	0.2893
<b>Funnel</b>	36 (30.25)	19 (29.69)	34 (30.91)	26 (31.33)	24 (36.92)	0.8962

No statistical differences were observed in NPC diameters for upper, middle and lower levels between the different ages (Table 2). But significant differences were observed in length (p = 0.0003); people over 60 years presented a longer canal (13.32 mm) than the group of 18–30 years (12.11 mm, p = 0.0010), while people of 40–50 years also had significantly longer canals in comparison with the group of 18–30 years (p = 0.0030).

**Table 2. Comparisons of the canal’s dimensions, including length and width, and analyze potential changes between age groups**

	Age groups Mean (Std Dev)					P Pairwise comparisons
	18-30	31-40	40-50	51-60	more than 60	
Upper Border	1.74 (0.64)	1.86 (0.85)	1.77 (0.70)	1.81 (0.79)	1.85 (0.91)	0.7869
Middle Level	1.76 (0.61)	1.65 (0.81)	1.70 (0.65)	1.93 (0.80)	1.77 (0.67)	0.1354
Lower Border	2.42 (0.86)	2.36 (1.12)	2.43 (0.92)	2.59 (1.00)	2.61 (0.95)	0.4145
Length of NPC/ Sagittal Plane	12.11 (1.74)	12.54 (1.81)	13.07 (2.40)	12.50 (1.80)	13.32 (2.20)	0.0003 more than 60 >18-30 (p=0.0010) 40-50 >18-30 (p=0.0030)

Accuracy of AI model:

During training, Class 2 performed best, with a Dice score and F1 score of 0.531, and high recall (0.682), indicative of good sensitivity. Class 1 showed the lowest performance (Dice and F1: 0.219), corresponding to inaccurate segmentation. Class 3 demonstrated high precision, but low recall as the model is probably had difficulty with the number of true instances. Class 4 was also partially labeled and attained a balanced precision (0.484), recall (0.576) and F1 = 0.434 (Table 3).

Table 3. Performance Metrics of the AI Model for Each Class During Training Phase

Class	Dice Score	Accuracy	Precision	Recall	F1 Score
Class 1	0.219	1.198	0.3	0.178	0.219
Class 2	0.531	1.198	0.489	0.682	0.531
Class 3	0.274	1.199	0.538	0.213	0.274
Class 4	0.434	1.198	0.484	0.576	0.434

For the testing phase, the AI model achieved the best result with Class 3 (Dice: 0.868, Accuracy: 1.000), demonstrating strong segmentation performance. Class 1 was also good results (Dice: 0.579, Accuracy: 0.999). Class 2 presented moderate results (Dice: 0.368) and Class 4 the less accurate one (Dice: 0.263), and was the most difficult to be determined. In summary, the model gave high accuracy and good segmentation of structures (Table 4).

Table 4. AI Model Performance Metrics per Class During Testing Phase

Class	Dice Score	Accuracy
Class 1	0.579	0.999
Class 2	0.368	0.997
Class 3	0.868	1.000
Class 4	0.263	0.998

## DISCUSSION

The position and contents of the NPC are of significant clinical interest, particularly in dental implantology, maxillofacial surgery, and local anesthesia administration. Understanding the morphology, variations, and dimensions of the NPC is essential for avoiding complications during surgical procedures in the anterior maxillary region and for improving surgical outcomes <sup>9</sup>.

The aim was to include both subjects in nearly all age categories up to advanced age in order to describe the effect of bone remodeling, with regard to age differences in anatomical dimensions, and also application an AI-based U-Net model for automated NPC segmentation. The model showed high accuracy, especially with clear canal shapes. Integrating AI with CBCT can improve diagnostic accuracy, enhance pre-surgical planning, and support personalized treatment in oral and maxillofacial surgery.

The observation of no differences in NPC shapes between age groups was in agreement with this research ( $P > 0.05$ ). The commonest shapes were cylindrical and funnel in general agreement with those of Görürgöz and Öztaş (2021)<sup>2</sup> and Yadav *et al.* (2025)<sup>10</sup> who also

identified these as the predominant shapes in the sagittal CBCT images. The hourglass shape had a decrease with age, which is consistent with Soman (2024)<sup>11</sup>, explaining this relationship via age-related remodeling, but no statistical significance was found in our results. The funnel shape of NPC tended to be similar among the age groups in our data which are supported by the studies of Alhumaidi *et al.* (2024)<sup>12</sup> and Hakbilen and Magat (2018)<sup>13</sup> who could not find a strong relationship between age and funnel-shaped NPC.

The age-related differences analysis revealed no statistical difference between canal width at the three levels of upper, middle and lower ( $p > 0.05$ ), which is similar to Bornstein *et al.* (2011b)<sup>14</sup> and Bajoria *et al.* (2018)<sup>15</sup> who found no relationship between age and canal width. However, NPC length was significantly longer in older ( $p = 0.0003$ ) subjects, in line with previous data. These findings are in agreement with Costa *et al.* (2019)<sup>16</sup> and Alotaibi *et al.* (2018)<sup>17</sup> who demonstrated that aging is related to increased canal lengthening, probably related to the maxillary bone and changes in the canal angulation as the aged, and greater apical scalloping as the aging process, when occurs at the expense of maxillary alveolar bone loss due to the natural process resulting from tooth loss, periodontal disease or general bone remodeling. This

may in turn result in inferior shift of the nasal floor and incisive foramen, thus lengthening the measured length of the NPC. Unlike Soman (2024)<sup>11</sup> NPC length determined did not vary significantly amongst the age, which was similar to the work of Al-Amery *et al.* (2015)<sup>18</sup> and Alasmari (2023)<sup>19</sup>.

However, most of these earlier investigations relied entirely on manual measurements, which are time-consuming and subject to observer variability. Recent advances in artificial intelligence (AI) have enabled automated image analysis in dental radiology.

In this work, U-Net achieved the highest Dice score on Class 2, 0.531, and recall rate, 0.682 in training phase. Classes 1 and 3 exhibited lower accuracy and recall. Such results are consistent with previous observations of Jiangtao *et al.* (2025)<sup>20</sup> and Pan *et al.* (2025)<sup>21</sup>, where it is found that the clear structure works well while the small or non-clear region does not work well.

The U-Net yielded the best classification results for Class 3 in testing phase (Dice: 0.868, accuracy: 1.000), with clear structure segmentation like study of Pan *et al.* (2025)<sup>21</sup>. Class 1 also had a good performance (Dice: 0.579), which was consistent with Sun *et al.* (2024)<sup>22</sup>, which supports that U-Net generalizes well on separate, easily identifiable organ systems.

For the testing phase, this study found that the U-Net generated an impressive global accuracy of 99%, which gives a high level of evidence for the effectiveness of the U-Net in multi-organ segmentation of complex images. The achieved accuracy is of particular significance since the model has been designed to detect simultaneously four classes, some of which might represent complex or subtle anatomical components.

Deniz *et al.* (2025) demonstrated the potential of deep learning algorithms such as YOLO for NPC segmentation and classification of furcation status, improving diagnostic efficiency<sup>23</sup>. Despite this progress, the application of AI for detailed morphological assessment of the NPC remains limited, with most existing methods relying on conventional threshold-based segmentation, which often struggles with complex anatomical structures. Our study addresses this gap by implementing a U-Net-based deep learning framework to automatically segment the NPC from CBCT scans. By leveraging a dataset with balanced representation across

age and gender groups, this approach improves segmentation accuracy, reduces manual labor, and minimizes observer bias. This methodological advancement provides a more consistent and reproducible analysis compared to traditional techniques. Furthermore, our integration of AI with morphological classification represents a step forward in creating standardized and scalable evaluation methods for clinical and research applications.

In summary, though earlier works were helpful in the understanding of NPC anatomy, those studies had been limited by being manual and using fewer subjects. Our approach introduces novelty by combining AI based segmentation with CBCT imaging for a complete and faster assessment of the NPC, which may contribute to serve as new exploration in applications on craniofacial diagnostics and surgical planning.

### Limitations

This retrospective study was limited by its reliance on pre-existing CBCT scans. Manual image annotation could introduce human error, and variations in scan quality may have influenced measurements and AI performance. Future multi-center studies with larger datasets are recommended.

### CONCLUSION

In conclusion the CBCT examination was useful for evaluation of the shape and size of the NPC. U-Net model-based segmentation with AI demonstrated a high degree of accuracy, especially for well-defined canal shapes. Thus, integrating CBCT with deep learning can help in improving diagnostic accuracy and facilitate safer planning of treatments.

### Recommendations

Future research should include larger, multi-center datasets to improve the accuracy and generalizability of findings. Automated annotation methods and advanced AI models are recommended to reduce human error and enhance segmentation performance.

### DECLARATIONS

**Funding:** This research received no external funding.  
**Conflict of Interest:** The authors declare no conflict of interest.  
**Acknowledgments:** None.

## REFERENCES

1. Erekosima B, Robinson E, Horsfall A, Didia M, Israel JTNHJ. Radio-Anatomical Evaluation of the Nasopalatine Canal and its Clinical implication: Radio-Anatomical Evaluation of the Nasopalatine Canal and its Clinical implication. *The Nigerian Health Journal*. 2024;24(3):1559-65.
2. Görürgöz C, Öztaş BJFm. Anatomic characteristics and dimensions of the nasopalatine canal: a radiographic study using cone-beam computed tomography. *Folia morphologica*. 2021;80(4):923-34.
3. Jacobs R, Lambrechts I, Liang X, Martens W, Mraiwa N, Adriaensens P, et al. Neurovascularization of the anterior jaw bones revisited using high-resolution magnetic resonance imaging. *Oral Surgery, Oral Medicine, Oral Pathology, Oral Radiology, and Endodontology*. 2007;103(5):683-93.
4. Chatzipetros E, Tsiklakis K, Donta C, Damaskos S, Angelopoulos CJD. Morphological assessment of nasopalatine canal using cone beam computed tomography: A retrospective study of 124 consecutive patients. *Diagnostics (Basel)*. 2023;13(10):1787.
5. Al-Ghurabi ZH, Al-Bahrani ZMJJoCS. Radiographic assessment of nasopalatine canal using cone beam computed tomography. *Journal of Craniofacial Surgery*. 2020;31(1):e4-e6.
6. Weiss R, Read-Fuller AJDj. Cone beam computed tomography in oral and maxillofacial surgery: an evidence-based review. *Dentistry journal*. 2019;7(2):52.
7. Chen Z, Chen S, Hu F. CTA-UNet: CNN-transformer architecture UNet for dental CBCT images segmentation. *Physics in medicine and biology*. 2023;68(17).
8. Yin XX, Sun L, Fu Y, Lu R, Zhang Y. U-Net-Based Medical Image Segmentation. *Journal of healthcare engineering*. 2022;2022:4189781.
9. Torres MGG, de Faro Valverde L, Vidal MTA, Crusoé-Rebello IMJRCdE. Trifid nasopalatine canal: case report of a rare anatomical variation and its surgical implications. *Revista Cubana de Estomatología*. 2016;53(2):67-70.
10. Yadav U, Shenoy N, Ahmed J, Sujir N, Archana M, Gupta A. Assessment of variations in the nasopalatine canal on CBCT: considerations from an anatomical. *Jour of periodont. & implant science*. 2024.
11. Soman C. Assessment of the Nasopalatine Canal Length and Shape Using Cone-Beam Computed Tomography: A Retrospective Morphometric Study. *Diagnostics (Basel, Switzerland)*. 2024;14(10):973.
12. Alhumaidi AM, Aseri AA, Alahmari MMM, Adawi HA, Aldhorae K, Gadah TS, et al. Morphological and Dimensional Analysis of the Nasopalatine Canal: Insights from Cone-Beam Computed Tomography Imaging in a Large Cohort. *Medical science monitor : international medical journal of experimental and clinical research*. 2024;30:e944424.
13. Hakbilen S, Magat G. Evaluation of anatomical and morphological characteristics of the nasopalatine canal in a Turkish population by cone beam computed tomography. *Folia morphologica*. 2018;77(3):527-35.
14. Bornstein MM, Balsiger R, Sendi P, von Arx T. Morphology of the nasopalatine canal and dental implant surgery: a radiographic analysis of 100 consecutive patients using limited cone-beam computed tomography. *Clinical oral implants research*. 2011;22(3):295-301.
15. Bajoria AA, Kochar T, Sangamesh N, Mishra S, Rout P, Sonthalia AJOJoS. Nasopalatine canal revisited: An insight to anterior maxillary implants. *Scientific Research* 2018;8(01):1.
16. Costa EDD, Nejaim Y, Martins LAC, Peyneau PD, Ambrosano GMB, Oliveira ML. Morphological Evaluation of the Nasopalatine Canal in Patients With Different Facial Profiles and Ages. *Journal of oral and maxillofacial surgery : official journal of the American Association of Oral and Maxillofacial Surgeons*. 2019;77(4):721-9.
17. Alotaibi MK, Alansari MA, Alqahtani JM, Alduhaymi AA, Assari A, Baseer MAJJoOH, et al. Evaluation of Greater Palatine Foramen and Incisive Canal Foramen among Saudi Patients using Cone Beam Computed Tomography Scans. *JOralHealth* 2018;12(2).
18. Al-Amery SM, Nambiar P, Jamaludin M, John J, Ngeow WCJPo. Cone beam computed tomography assessment of the maxillary incisive canal and foramen: considerations of anatomical variations when placing immediate implants. *journalsplosorg*. 2015;10(2):e0117251.
19. Alasmari D. Morphometric Evaluation of Morphological Variations of the Nasopalatine Canal: A Retrospective Study Using Cone-beam Computed Tomography. *The journal of contemporary dental practice*. 2023;24(9):660-7.
20. Jiangtao W, Ruhaiyem NIR, Panpan FJIIP. A Comprehensive Review of U-Net and Its Variants: Advances and Applications in Medical Image Segmentation. *IETImageProcessin*. 2025;19(1):e70019.
21. Pan P, Zhang C, Sun J, Guo LJSR. Multi-scale conv-attention U-Net for medical image segmentation. *Scientific reports*. 2025;15(1):12041.
22. Sun G, Pan Y, Kong W, Xu Z, Ma J, Racharak T, et al. DA-TransUNet: integrating spatial and channel dual attention with transformer U-net for medical image segmentation. *Frontiers in bioengineering and biotechnology*. 2024;12:1398237.
23. Deniz HA, Bayrakdar İŞ, Naıçacı R, Orhan KJOR. Segmentation of the nasopalatine canal and detection of canal furcation status with artificial intelligence on cone-beam computed tomography images. *Oral radiology*. 2025:1-11.